J. Am. Soc. Mass Spectrom. (2017) 28:2677–2685
DOI: 10.1007/s13361-017-1791-z

RESEARCH ARTICLE

What Hinders Electron Transfer Dissociation (ETD) of DNA Cations?

Yvonne Hari, Christian J. Leumann, Stefan Schürch

Department of Chemistry and Biochemistry, Freiestrasse 3, 3012 Bern, Switzerland

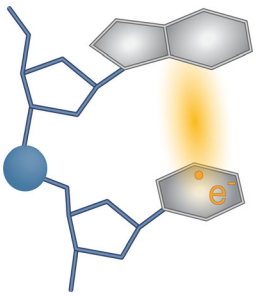

Abstract. Radical activation methods, such as electron transfer dissociation (ETD), produce structural information complementary to collision-induced dissociation. Herein, electron transfer dissociation of 3-fold protonated DNA hexamers was studied to gain insight into the fragmentation mechanism. The fragmentation patterns of a large set of DNA hexamers confirm cytosine as the primary target of electron transfer. The reported data reveal backbone cleavage by internal electron transfer from the nucleobase to the phosphate linker leading either to *a*•/*w* or *d*/*z*• ion pairs. This reaction pathway contrasts with previous findings on the dissociation processes after electron capture by DNA cations, suggesting multiple, parallel dissociation channels. However, all these channels merely result in partial fragmentation of the precursor ion because the charge-reduced DNA radical cations are quite stable. Two hypotheses are put forward to explain the low dissociation yield of DNA radical cations: it is either attributed to non-covalent interactions between complementary fragments or to the stabilization of the unpaired electron in stacked nucleobases. MS^3 experiments suggest that the charge-reduced species is the intact oligonucleotide. Moreover, introducing abasic sites significantly increases the dissociation yield of DNA cations. Consequently, the stabilization of the unpaired electron by π–π-stacking provides an appropriate rationale for the high intensity of DNA radical cations after electron transfer.

Keywords: ETD, DNA radical cations, Sugar-modified DNA, Dissociation mechanism

Received: 29 June 2017/Revised: 18 August 2017/Accepted: 18 August 2017/Published Online: 20 September 2017

Introduction

Tandem mass spectrometric experiments aim at the sequence and structure elucidation of complex biomolecules such as peptides and nucleic acids. Collision-induced dissociation (CID) is the most widely applied technique for MS/MS sequencing of oligonucleotides. In DNA, CID results in base loss and subsequent cleavage of the 3'-C–O phosphodiester bond, yielding *a* - B and *w* fragment ions according to the nomenclature by McLuckey et al. [1]. However, collisional activation also triggers nonspecific dissociation pathways, such as the loss of water or nucleobases, and secondary reactions that produce internal fragments. The parallel dissociation pathways of DNA and RNA are described in two comprehensive reviews [2, 3]. The combination of multiple CID reaction channels increases the complexity of the product ion spectrum and reduces the intensity of sequence-specific backbone fragments. This encourages the use of alternative, radical-based activation techniques, such as electron transfer dissociation (ETD), negative electron transfer dissociation (NETD), electron capture dissociation (ECD), electron detachment dissociation (EDD), and electron photodetachment dissociation (EPD). Various authors showed that no internal fragments and little nonspecific nucleobase loss are observed upon ECD [4–6], ETD [7], and EDD [8, 9] of DNA oligonucleotides. For all radical activation methods, *a*•, *d*, *w*, and *z*• are the most frequently observed product ions.

The gas-phase dissociation of odd-electron DNA species was first reported by McLuckey et al. [10], who observed the formation of *a* - B and *w* ions from radical anions created by ion–ion reactions with CCl_3^+ and $Xe^{+\bullet}$. More recent NETD studies revealed the generation of non-complementary *d*/*w* ion series and full sequence information from radical anions of 2'-modified nucleic acids [11]. The authors propose that the radicals are formed by the removal of an electron from the deprotonated phosphate linkers. The relocation of the radical site then induces the cleavage of the phosphodiester backbone. By contrast, the oxidation by EDD and EPD was shown to be a nucleobase-dependent process. For the four hexanucleotides dA_6, dC_6, dG_6, and dT_6, different electron detachment [9] and electron photodetachment [12] efficiencies were measured.

Correspondence to: Stefan Schürch; *e-mail:* stefan.schuerch@dcb.unibe.ch

Similar nucleobase dependence was reported for the reduction of DNA cations by electron capture [13] or electron transfer [7]. The comparison of pyrimidine pentanucleotides demonstrates that electron capture is a charge-directed process in which the odd electron is initially captured by the protonated nucleobase [6]. Chan et al. propose that the electron is captured by the nucleobase, whereafter the transfer of a hydrogen atom from the reduced base to the neighboring phosphate linker induces the cleavage of the 5'-C–O bond and gives rise to *d*/*z*• ions. The formation of the *a* - B/*w* ion pair is presumably initiated by the loss of a neutral nucleobase upon reduction. For electron transfer dissociation, the fragmentation mechanism has not been elucidated yet. Although the process is likely to produce the same type of radical cations as ECD, the herein presented data give strong evidence that the detected backbone fragments are not formed by the same mechanism as proposed for ECD.

The formation of stable radical cations is among the most significant challenges for the characterization of biopolymers by electron capture dissociation and electron transfer dissociation. While both ECD and ETD have become appreciated techniques for peptide sequencing that induce the cleavage of the N–C_α bond in the backbone, limited yields of fragment ions were determined for proteins. High-intensity peaks whose *m/z* values correspond to charge-reduced species $[M + nH]^{(n-1)+\bullet}$ were detected instead. In a series of ECD experiments, McLafferty and co-workers demonstrated that preheating of the selected precursor, collisions with the background gas, as well as IR irradiation after electron capture significantly increase the fragmentation yield and reduce the intensity of the $[M + nH]^{(n-1)+\bullet}$ ions [14–16]. Consequently, it is assumed that electron-ion recombination triggers backbone cleavage, but the generated product ions do not separate. Complementary fragments remain linked by non-covalent interactions. In other words, the high-intensity $[M + nH]^{(n-1)+\bullet}$ peaks correspond to aggregates of fragments and not to the intact, charge-reduced protein.

The rationale of non-covalently connected fragments was transferred from proteins to nucleic acids. ECD of the DNA homomers dA_6 and dG_6 revealed a significantly reduced degree of backbone cleavage compared to dC_6, which was attributed to intramolecular hydrogen bonds that prevent the product ions from separating [5, 17]. There is ample experimental and computational data that demonstrate intramolecular phosphate–nucleobase or phosphate–phosphate hydrogen bonds [18–21]. However, the number of possible intramolecular hydrogen bonds in a DNA hexamer is limited, and it is questionable if the non-covalent bonds between complementary ECD fragments of large proteins are comparable to the interactions in short oligonucleotides.

Herein, we propose an alternative explanation for the high stability of DNA radical cations. The dissociation yield after electron transfer was found to be augmented for sugar-modified homo-DNA oligonucleotides. As shown in Figure 1, 2',3'-di-deoxyglucopyranose substitutes the deoxyribose in homo-DNA, resulting in increased spatial separation of the nucleobases. In DNA, the unpaired electron is proposed to be stabilized by π–π-stacking interactions of adjacent nucleobases, while the separation of nucleobases in homo-DNA prevents efficient stabilization of the electron and favors backbone cleavage. This hypothesis is supported by MS^3 data on charge-reduced DNA radical cations and ETD experiments on oligonucleotides harboring abasic sites.

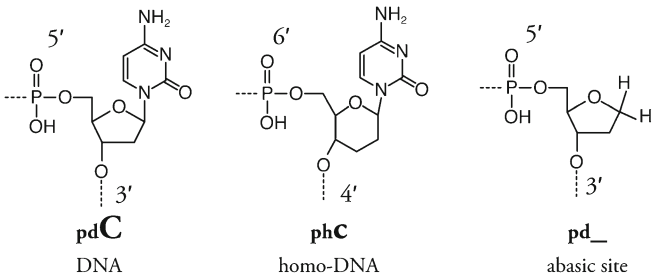

Figure 1. The structures of DNA, homo-DNA, and abasic sites. The DNA homologue homo-DNA harbors an additional methylene group between C1' and C2' of the sugar moiety. In the abasic site, the C1' atom carries a second hydrogen atom instead of a nucleobase

Experimental

Oligonucleotides, Chemicals, and Solvents

A list of all oligonucleotides used is compiled in Table 1. The DNA hexamers were purchased from Microsynth (Balgach, Switzerland). The RNA hexamers were obtained from TriLink Biotechnologies (San Diego, CA, USA), and the methylphosphonate modified DNA hexamers from Eurogentec S.A. (Seraing, Belgium). Two DNA hexamers were used containing abasic sites (_), i.e., deoxyribose moieties carrying two hydrogen atoms at the C1' atom. The oligonucleotides with abasic sites, d(TAGC_A) and d(TA_C_A), were obtained from TriLink Biotechnologies. All oligonucleotides were purchased as ammonium salts and used without further purification. They were dissolved in HPLC grade water to yield 1 mM stock solutions. The fully modified homo-DNA oligonucleotides h(ccggtt), h(ttggcc), and h(gccta) as well as the DNA/homo-DNA mixmers 5'-CAcgt-4', 6'-cacGT-3', and 6'-gccTA-3' were synthesized according to a previously published procedure [22]. The pentamer h(gccta) carries an additional 6'-hexylamine linker. Prior to analysis, the oligonucleotides were diluted to a final concentration of 10 µM in a 1:1 water:MeOH solvent containing 0.5% formic acid. Fluka HPLC grade water and formic acid were purchased from Sigma-Aldrich (Sigma-Aldrich Chemie GmbH, Buchs, Switzerland), HPLC grade methanol was purchased from Fisher Scientific (Loughborough, UK).

Mass Spectrometry

All mass spectrometric experiments were performed on a LTQ Orbitrap Velos instrument (Thermo Fisher Scientific, Bremen, Germany) equipped with an ESI source. The experiments were

Table 1. List of All Oligonucleotides and ETD Product Ions of Triply Charged Precursors M^{3+}

	Sequence	$a_1^{\bullet}$/ w_5	$a_2^{\bullet}$/ w_4	$a_3^{\bullet}$/ w_3	$a_4^{\bullet}$/ w_3	$a_5^{\bullet}$/ w_1	d_1/ $z_5^{\bullet}$	d_2/ $z_4^{\bullet}$	d_3/ $z_3^{\bullet}$	d_4/ $z_2^{\bullet}$	d_5/ $z_1^{\bullet}$	M
DNA	CCGGTT	0.4										85.4
		13.1	0.5									
	TTGGCC				0.1					1.9	**8.3**	79.4
										2.2	**6.9**	
	TTCCGG								0.6			97.8
				0.1					0.5			
	CGTGCT	1.2								1.6		85.3
		8.7								2.6		
	TCGTGC										**17.5**	58.8
								0.7			**21.2**	
	CGGCTT	0.3						<0.1	2.6			87.0
		4.6	<0.1						2.6			
	CCGTCA	2.3	0.6			0.1	<0.1			0.6	0.2	83.6
		7.7	1.8			0.3	0.2			0.6	0.1	
	CAGACT	2.3						<0.1		2.7		80.7
		4.4	0.1	0.1						3.4		
	CGACGT	0.6						0.1	1.2			88.9
		4.8						<0.1	1.2		<0.1	
	AGAGAT	<0.1									0.1	97.6
		0.2	0.1		<0.1			<0.1				
	AGTCGC								<0.1	<0.1	**17.9**	68.7
		0.2	<0.1							<0.1	**11.2**	
	TGCTAG			1.1				0.4				93.9
				1.8				0.1				
	TAGCGA								0.2			97.7
			0.1						0.5		0.2	
	TAGC__A		<0.1	0.1	0.8	<0.1		<0.1	**8.8**	2.0	0.2	66.3
		<0.1	0.1	0.3	2.2	2.8		<0.1	**9.2**		0.2	
	TA__C__A		0.2	0.1	2.2			**6.0**	**9.7**	3.5	0.2	49.9
		0.1	0.7	4.7	**6.8**	**5.3**			**9.5**		0.1	
RNA	r(CCGGUU)											94.3
		3.4	2.3									
	r(GAUCGU)		0.2			<0.1				2.0		95.1
		0.1	0.5							1.7	0.1	
	r(UGCUAG)			0.2				**7.7**				81.3
			0.2	0.9	2.2			4.7				
Methylphosphonate	C*C*G*G*T*T	1.6	2.0	0.1			0.1	<0.1				89.4
		4.0	2.0	0.1			0.1	0.2				
	C*C*GG*T*T	0.5	2.2				0.1	0.1		<0.1		90.3
		3.2	2.6	0.1			0.1	<0.1				
	C*C*G*GT*T	0.6	1.3	<0.1		<0.1		<0.1		<0.1	<0.1	93.0
		2.0	1.6	0.1	<0.1		0.1	0.1				
	m(CCGGUU)	1.6	1.0			0.3				0.1		76.0
		19.0	1.8									
	m(CC*G*GUU)	0.3	1.8	<0.1					0.1			89.1
		6.0	2.5	0.2								
homo-DNA/DNA and homo-DNA	ccggtt	**40.4**										25.7
		31.7										
	ttggcc					0.6				**9.1**	**15.3**	60.5
						0.7				**6.9**	**5.7**	
	gccta	<0.1	**6.1**	4.3	0.2	-	**6.9**	**5.2**	<0.1	<0.1	-	54.5
		-	<0.1	**6.8**	**7.8**	0.3	-	2.8	3.5	<0.1		
	gcacgt	0.7	2.0		0.2			2.5	3.4			50.4
		7.3	2.8		1.6			0.8	2.3			
	gccTA		**22.6**	2.4		-	2.4	**9.2**			-	21.1
		-		**27.4**	**5.3**		-	2.4	**5.5**			
	cacGT	**17.7**	0.1	1.0		-		**12.9**	0.1	0.2	-	23.9
		-	**27.0**	0.3	**6.1**		-	<0.1	**8.9**	<0.1		
	CAcgt			3.2		-		**29.6**			-	38.8
		-	1.7		**9.4**		-		**17.0**			

Abbreviations: methylphosphonate linkers: *, RNA: r, 2'-O-methylribose: m, abasic sites: _, homo-DNA nucleotides: small letters. For each precursor, the intensities of the backbone fragments were normalized to the total product ion intensity for semiquantitative classification

performed in the positive mode applying the following source parameters: spray voltage 3.2 kV, capillary temperature 180 °C, sheath gas flow rate 5, and S-lens RF level 67%. Mass spectra were acquired in the FTMS mode from *m/z* 200 to 2000 with the mass resolution set to 100,000. ETD experiments were performed using fluoranthene as electron donor. Fluoranthene radical anions were produced in the reagent ion source under the following conditions: emission current 50 μA, electron energy 70 eV, source temperature 160 °C, CI gas pressure 7.8 psi, and reagent vial temperature 90 °C. The activation time for ETD was set to 100 ms. For all ETD experiments, the triply charged oligonucleotide $[M + 3H^+]^{3+}$, symbolized as M^{3+}, was isolated as precursor with a ±2 *m/z* selection window. In MS^3 experiments, the doubly charge-reduced $M^{+\bullet\bullet}$ ion was isolated in the HCD collision cell and subjected to high-energy collision-induced dissociation using nitrogen as collision gas. The Xcalibur Software Suite including QualBrowser ver. 2.2 (Thermo Fisher Scientific) was used for data processing. Data analysis was supported by the OMA and OPA software tool [23]. For quantitative comparison of the obtained product ions, the total product ion intensity was determined by adding the intensities of $M^{+\bullet\bullet}$, $M^{2+\bullet}$, $[M - BH]^{+\bullet\bullet}$, $a^{\bullet}$, *d*, *w*, and $z^{\bullet}$ ions. All product ion intensities indicated in the text, in figures, and in Table 1 are normalized to the total product ion intensity of the corresponding spectrum.

Results and Discussion

Selective Reduction of Cytosine

Electron transfer (ET) to triply charged DNA hexamer cations results in the reduction of the charge state producing the radical species $M^{2+\bullet}$ and $M^{+\bullet\bullet}$ (short for $[M + 3H^+ + e^-]^{2+\bullet}$ and $[M + 3H^+ + 2e^-]^{+\bullet\bullet}$). Although these radicals exhibit remarkable stability in the gas-phase, their formation can be followed by backbone cleavage or nucleobase loss. For a large set of oligonucleotides, the signal intensities of all detected backbone fragments normalized to the total product ion intensities are listed in Table 1. The cleavage of the C–O bond on the 5'-side of cytosines is preferred, which suggests favored electron transfer to this nucleobase. Overall, the reduction of nucleobases followed the order C > A > G > T. The preference for cytosine arises from the high proton affinity in conjunction with the highly exothermic ion–electron recombination, as calculations by Chan et al. on ECD indicate [6]. The selective reduction of cytosine resembles previous findings on ECD of

poly-pyrimidines [6] and is described herein for the first time for DNA oligonucleotides containing all four nucleobases. The trend contrasts with collision-induced activation of DNA, which is characterized by preferred cleavage at the purine nucleobases. Therefore, ETD or ECD is expected to provide sequence information complementary to CID for C-rich sequences and thereby contribute to identifying methylated cytosines in natural nucleic acids. When multiple cytosines are present in the DNA hexamer, cleavage next to the terminal bases is clearly preferred over the cleavage next to the internal cytosine. This effect was observed for 5'-terminal cytosines in hexamers, which result in the formation of w_5^+ ions, as well as 3'-terminal cytosines, which give rise to abundant d_5^+ ions (see Figure 2). This trend underlines that electron transfer is a charge-directed process as the protons are likely to be pushed to the terminal nucleobases by Coulombic repulsion.

Nucleobase loss is characterized by the same order of preference as backbone cleavage, identifying it as an electron-induced process rather than a spontaneous reaction triggered by vibrational or rotational energy in the oligonucleotide. Purines are only ejected with similar probability as cytosine when located in a terminal position. For the two isomers d(TTGGCC) and d(TTCCGG), for example, the loss of cytosine is preferred in the first case, whereas similar propensities for the loss of guanine and cytosine were observed in the second oligonucleotide comprising a terminal guanine. In agreement with previous ECD studies [4], the odd electron on the nucleobase induces the homolytic scission of the N-glycosidic bond, resulting in the loss of neutral nucleobases. $[M - BH]^{2+\bullet}$ and $[M - BH]^{+\bullet\bullet}$ fragments evidence neutral base loss from the singly and doubly reduced oligonucleotides. For quantitative comparison of parallel reaction pathways, the intensity of product ions was normalized to the total intensity of all product ions in the spectrum, i.e., the cumulative intensity of charge reduced cations, base loss products, and backbone fragments. Nucleobase loss accounts for only 1% – 3% of the total signal intensity in the product ion spectrum of DNA hexamers, which is an insignificant contribution compared with charge reduction and backbone cleavage. No backbone fragments missing nucleobases were observed (e.g., no *a* - B fragments), which suggests that base loss and backbone cleavage are independent processes.

Fragmentation Mechanism of d/z• Ion Pairs in DNA

The reduction of nucleobases, especially cytosines, by electron transfer gives rise to backbone cleavage, the main backbone fragments being *a*•/*w* and *d*/*z*• ion pairs. This pattern is in agreement with previous studies combining electron transfer and collisional activation [7], and compares well with the results obtained by ECD of DNA cations [4]. While this similarity may suggest identical dissociation pathways, the presented ETD data contradict the previously published ECD dissociation mechanism. Chan et al. propose that the *d*/*z*• ion pair is formed by the transfer of a hydrogen atom from the reduced nucleobase to the 5'-phosphate group, which leads to the homolytic scission of the 5'-C–O bond [6]. Applied to a 3'-terminal cytosine in a triply charged precursor such as d(TTGGCC), this mechanism leads to the formation of a doubly charged d_5^{2+} ion and a neutral *z*• radical. Our data consistently show, however, that the complementary ions are both observed as singly charged species of equal intensity, i.e., d_5^+ and $z_1^{+\bullet}$ ions are detected (see Figure 2). The occurrence of the $z_1^{+\bullet}$ ion proves that the terminal nucleobase retains its proton. A similar reasoning applies to short z ions with 3'-terminal thymines, such as $z_2^{+\bullet}$ in d(CGTGCT) or $z_3^{+\bullet}$ in d(CGGCTT). Owing to its low proton affinity, thymine is an unlikely protonation site and the positive charge in the *z*• radical cations

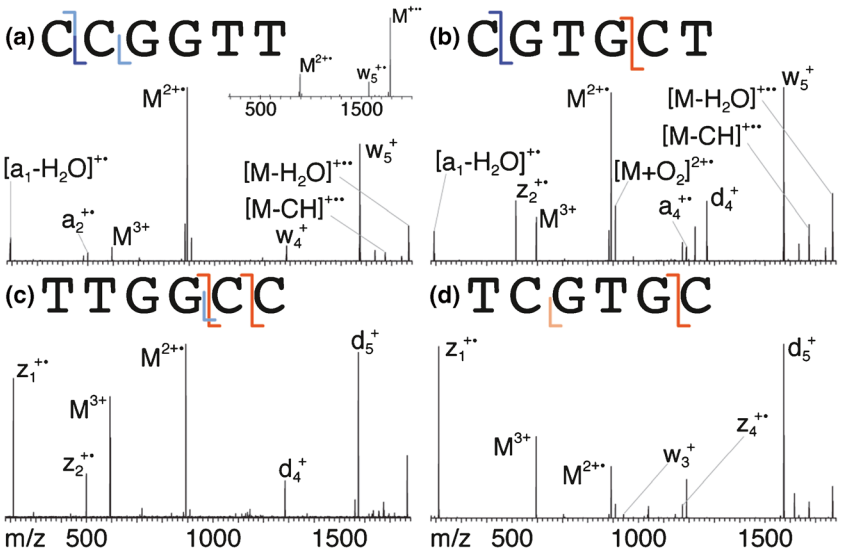

Figure 2. The ETD spectra of the triply charged DNA hexamers **(a)** CCGGTT, **(b)** CGTGCT, **(c)** TTGGCC, and **(d)** TCGTGC. In the schemes, the formation of a•/w and d/z• pairs are indicated with blue and orange lines, respectively. Pale colors indicate relative ion intensities <0.1%

must be localized on the cytosine, where it triggered the reduction in the first place. Consequently, backbone cleavage is not brought about by the transfer of a hydrogen atom but by electron transfer from the nucleobase onto the phosphate linker.

This process is rationalized by ab initio calculations on DNA damage by low-energy electrons presented by Simons and co-workers [24]. The authors describe internal electron transfer from the π*-orbital on the nucleobase to the σ*-orbital of the 3'-C–O bond. While the ab initio calculations were only performed for 3'-phosphate nucleotides, ETD experiments suggest that this explanation is also applicable to the 5'-C–O bond. After the internal electron transfer, the 5'-C–O bond is cleaved, resulting in an unpaired electron on the *z*• radical ion and a negative charge on the phosphate group (see Figure 3, bottom). The resulting *d* ion is therefore a zwitterion with one negative charge on the last phosphate group and two protons on separate nucleobases. Despite the Coulombic attraction between the negatively charged phosphate group on the d ion and the *z*• radical cation, MS^3 data give no evidence that the complementary ions are held together after their generation (see below). Internal proton transfer in the *d* ion may facilitate the separation of the fragments.

Backbone cleavage induced by the transfer of a hydrogen radical H•, while characteristic for ECD, constitutes a very minor reaction pathway in ETD experiments. The d_5^{2+} ion in the ETD spectrum of d(AGTCGC) and the d_1^+ ion generated from the triply charged d(CCGTCA) precursor give evidence for this process. The different fragmentation channels are most likely the consequence of lower ion–electron recombination energies upon electron transfer. Compared with the capture of free electrons in ECD, the recombination energy in ETD is reduced by the energy required to separate the electron from its carrier, here fluoranthene.

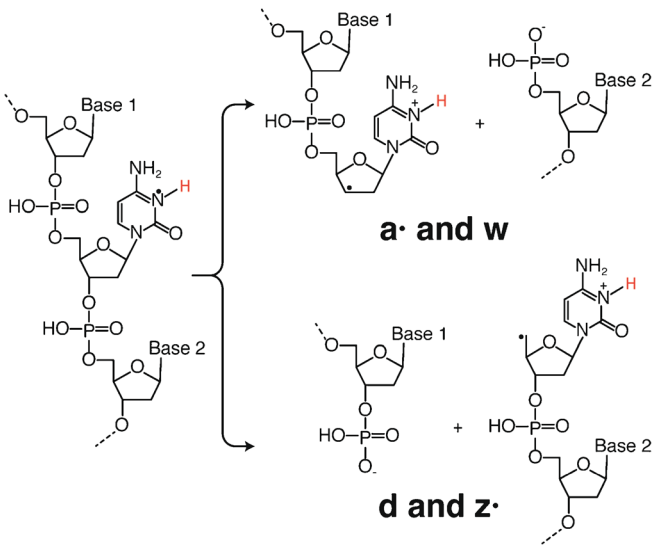

Figure 3. Dissociation products of ETD. Internal electron transfer induces the cleavage of the backbone at the 5'-C-O bond (top) or the 3'-C-O bond (bottom). The phosphate group on the resulting w-ion or d-ion carries a negative charge, whereas the nucleobase that was reduced in the initial step harbors a positive charge

The Formation of a•/w Ion Pairs

The cleavage of the 3'-C–O bond presents the second dissociation pathway yielding abundant backbone fragments. Previous mechanistic ECD studies suggest that the cleavage of this bond is induced by the loss of the nucleobase [6]. In the herein presented ETD experiments, where no *a* - B ions were observed, backbone cleavage appears to be independent of nucleobase loss. Presumably, the *a*•/*w* ion pair is likewise the product of internal electron transfer. As for the *d*/*z*• ion pair, the transfer of a hydrogen radical presents an alternative, minor pathway.

The formation of *a*•/*w* ion pairs is the dominant fragmentation pathway for oligonucleotides containing 5'-terminal cytosines and pairs of cytosines. In the product ion spectrum of d(CCGGTT) shown in Figure 2, for example, the w_5^+ ion is the base peak and the w_4^+ ion exhibits high intensity, while d_1^+ and $z_5^{+\bullet}$ ions are not observed. Backbone cleavage thus occurs at the 3'-C–O bond of both cytosines. With the exception of d(CCGGTT), however, the formation of *d*/*z*• pairs is preferred over the formation of *a*•/*w* pairs for internal cytosines. The preferred cleavage of the 5'-C–O bond rather than the 3'-C–O bond after the reduction of the cytosine is not fully understood at present. In reference to the proposed internal electron transfer, we hypothesize that the preference is due to energetic differences of the σ*-orbitals involved. This behavior contrasts with CID data on DNA cations, where the formation of *a* - B and *w* ions is observed. Consequently, ETD and CID experiments may be combined to pinpoint modifications within the phosphate linker.

The Effect of Structural Modifications on the Dissociation Mechanism

The proposed dissociation mechanism is independent of unique functional groups and is substantiated by MS/MS data for structural analogues of DNA. ETD experiments on the DNA oligonucleotide d(CCGGTT), the RNA oligonucleotide r(CCGGUU), and the methylphosphonate hexamer d(C*C*G*G*T*T) reveal identical fragmentation patterns for all three types of nucleic acids, namely the formation of $a_1^{+\bullet}/w_5^+$ and $a_2^{+\bullet}/w_4^+$ ion pairs (see Table 1). Cleavage after the terminal cytosine is also observed in the homo-DNA analogue h(ccggtt). Similarly, $z_1^{+\bullet}/d_5^+$ and $z_2^{+\bullet}/d_4^+$ ions were detected after ETD of d(TTGGCC) and h(ttggcc). Consequently, the mechanism of the backbone cleavage is not affected by structural modifications that conserve the phosphodiester linkage in the backbone, which confirms the proposed internal electron transfer.

In contrast to DNA and RNA oligonucleotides, the total intensity of backbone fragments generated from homo-DNA precursors is remarkably high. The signals of the backbone fragments yield up to 72% of the total product ion intensity, compared with 10%–20% dissociation yield in unmodified

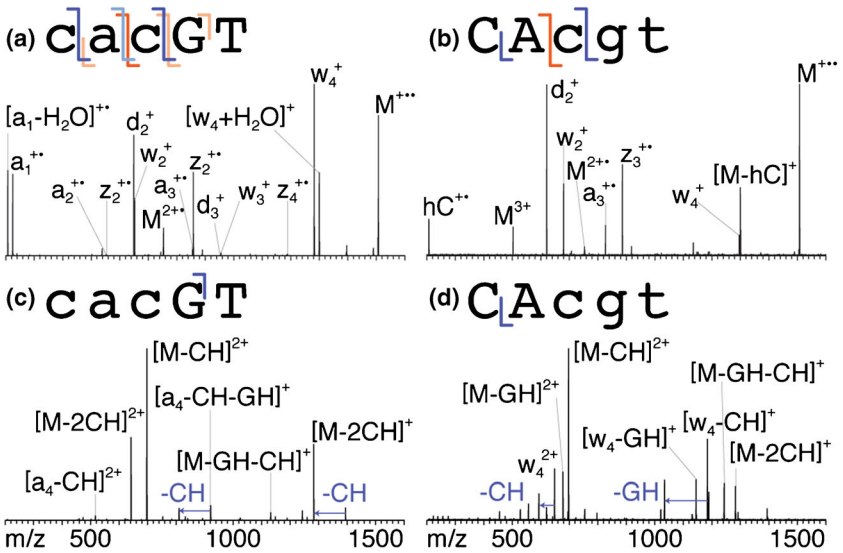

Figure 4. The ETD spectra of the triply charged DNA/homo-DNA mixmers **(a)** cacGT, and **(b)** CAcgt reveal preferred backbone cleavage at the modified sugar-moieties. This contrasts strongly with the fragmentation pattern observed in CID [**(c)** and **(d)** for doubly charged precursors], where nucleobase loss is dominant and only moderate backbone cleavage at the non-modified nucleotides is observed. The formation of a•/w and d/z• pairs are indicated with blue and orange lines in the schemes. Pale colors indicate relative ion intensities <0.1%

nucleic acids. The ETD fragmentation pattern of the three mixed DNA/homo-DNA pentamers ggcTA, cacGT, and CAcgt underlines the augmented backbone cleavage next to the homo-DNA sugar moieties (small letters) compared with deoxyribose nucleotides. This result is most remarkable for CAcgt, where the dC-nucleotide presents the most likely site for electron transfer. The terminal cytosine can be expected to carry one of the three positive charges to minimize the Coulombic repulsion of the three protons. However, as shown in Figure 4b, the w_4^+ ion is barely detected, while the d_2^+ and $z_3^{+\bullet}$ ions are the main fragmentation products. Evidently, backbone cleavage next to the internal, modified hc is preferred over backbone cleavage at the terminal dC nucleoside. The nucleobases are the same, suggesting identically efficient electron transfer from fluoranthene to dC and hc. Since the formation of abundant $M^{+\bullet\bullet}$ ions is observed for DNA as well as homo-DNA precursors, electron transfer is not the limiting factor for the fragmentation of unmodified nucleic acids. Instead, the augmented dissociation yield in homo-DNA must be due to less effective stabilization of the radical species.

The propensity for nucleobase loss from reduced homo-DNA cations is very small, contrasting strongly with the dissociation observed upon collisional activation, where homo-DNA cations were reported to exclusively undergo nucleobase loss but not backbone cleavage [25]. The characteristic reaction pathways are reflected by the spectra in Figure 4, showing ETD and CID spectra of DNA/homo-DNA mixmers. ETD leads to bond scission at the modified nucleotides, whereas CID exclusively triggers backbone cleavage in the DNA-part of the mixmers and induces nucleobase loss from the homo-DNA nucleotides. Consequently, the characterization of highly modified nucleic acids benefits from a diverse set of available techniques and encourages further ETD studies. Since the fragmentation mechanism is not affected by any of the modifications tested herein, radical activation is expected to provide sequence information complementary to CID for complex nucleic acids such as tRNAs harboring multiple types of modifications.

Stabilization of the Radical Cations

The stabilization of reduced oligonucleotides presents the main obstacle for DNA sequencing by radical activation methods. Though reported previously for ECD and ETD, the effect is poorly understood. Herein, two possible explanations for the high intensity of $M^{+\bullet\bullet}$ ions in the ETD spectra of DNA hexamers are presented and compared: either fragment ions are held together by non-covalent interactions after backbone cleavage (hydrogen bonding hypothesis), or the stabilization of the unpaired electron prevents the cleavage of the backbone (stacking hypothesis).

In essence, the hydrogen bonding hypothesis postulates that the high intensity signal labeled as $M^{+\bullet\bullet}$ does not arise from the intact, charge-reduced oligonucleotide, but from non-covalently connected complementary ion pairs, the mass of which is equal to the mass of the selected precursor. Such non-covalent interactions were found to persist in proteins after electron capture [15] and may also prevent the separation and detection of nucleic acid backbone fragments. Hydrogen bonding has been proposed to explain the low fragmentation yields observed in ECD experiments on the DNA homomers dC_6, dA_6, and dG_6. dA_6 was found to exhibit the most stable radical species of the three oligonucleotides, which was attributed to hydrogen bonds between the nucleobases and the phosphate linkers [17]. Incomplete sequence information in ECD spectra of dG_6 was similarly rationalized [4]. Hydrogen bonds formed

between phosphate linkers and purines in the *syn* conformation were also found to trigger increased backbone cleavage at G in RNA upon CID [26].

The first test to the hydrogen bonding hypothesis is the question whether H-bonds might similarly prevent the separation of backbone fragments in homo-DNA. CID data on homo-DNA oligonucleotides provide strong evidence for proton transfer from the backbone to the nucleobase. The release of neutral nucleobases from oligonucleotide anions and positively charged nucleobases from cations constitute major dissociation pathways of homo-DNA [25]. Consequently, the altered geometry of the modified sugar moiety does not preclude hydrogen bonding between the nucleobase and adjacent phosphate groups. The relative orientation of functional groups and the strength of non-covalent interactions may, however, be affected.

Assuming that complementary backbone fragments are held together by non-covalent interactions, they should readily separate upon collisional activation of the assembly. Therefore, MS^3 data were acquired for the DNA hexamer d(TAGCGA) by subjecting the $M^{+\bullet\bullet}$ ion to high-energy collision-induced dissociation (HCD). The relative intensities of $M^{+\bullet\bullet}$, $[M-BH]^{+\bullet\bullet}$ ions, and backbone fragments were determined at various activation regimes and normalized to the cumulative intensity of all ions in the MS^3 spectrum. Figure 5 illustrates the contribution of nucleobase loss and selected backbone fragments as a function of the collision energy. Backbone cleavage in the MS^2 step is only observed at the cytosine, giving rise to low-intensity d_3^+ and $z_3^{+\bullet}$ ions. In the MS^3 spectra, by contrast, they contribute less than 0.8% to the total product ion intensity. The most abundant product ions are CID-typical fragments generated by backbone cleavage at the guanines, namely a_3-B, a_5-B, w_3, and w_1 ions.

The onset of nucleobase loss in the MS^3 stage was observed at intermediate activation energies (25 eV), and backbone fragments were only detected at higher energies (47 eV). To reduce the intensity of the selected precursor by 50%, the collision energy had to be increased to 58 eV. This is comparable with the collision regime required to fragment the singly protonated dT_6 in the MS^2 mode, which was chosen as reference because the contribution of non-covalent interactions to the stability of this precursor is minimal. The product ions in the MS^3 spectrum of d(TAGCGA), therefore, arise from the cleavage of covalent bonds rather than the disruption of hydrogen bonds. In conclusion, the CID-typical fragmentation pattern and the high stability of the isolated precursor ion in the MS^3 step are in disagreement with the hydrogen bonding hypothesis. The presented data indicate that the base peak in ETD spectra of DNA hexamers indeed corresponds to the intact, reduced oligonucleotide rather than a non-covalently linked aggregation of backbone fragments.

The alternative explanation, the stacking hypothesis, proposes that the scarce generation of backbone fragments after electron transfer to DNA cations is due to the stabilization of the unpaired electron by nucleobase stacking. This rationale builds on ETD data of homo-DNA oligonucleotides, characterized by the elevated dissociation yields of fully and partly sugar-modified precursors. In homo-DNA, the additional methylene group between C1' and C2' leads to significant conformational changes that increase the distance between adjacent nucleobases. In crystal structures of homo-DNA duplexes, the distance between neighboring nucleobases measures up to 5.1 Å [27] (compared with 3.4 Å in DNA). The separation of the nucleobases in homo-DNA impedes efficient base stacking and promotes high dissociation yields in ETD experiments. By contrast, π–π-stacking in DNA is proposed to stabilize the unpaired electron and thus suppresses backbone cleavage. In ab initio studies, non-covalent interactions of stacked nucleobases were found to augment the energy barrier for the scission of the phosphodiester backbone by internal electron transfer [28]. The presented ETD data on homo-DNA give experimental evidence of this stabilizing effect.

The rationale is applicable to radical cations generated by other activation techniques such as ECD and possibly even to radical anions. Previous studies evidenced nucleobase-dependent oxidation of DNA anions by EDD and EPD [8, 9, 12, 13], creating long-lived, unpaired electrons on the nucleobases, which may be stabilized by nucleobase stacking.

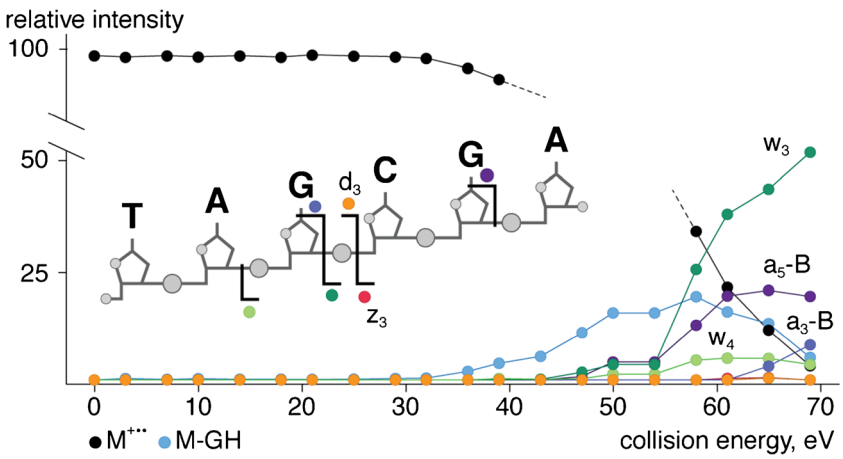

Figure 5. The normalized intensities of selected backbone fragments, nucleobase loss, and the precursor ion in the MS^3 spectrum of $M^{+\bullet\bullet}$ ion d(TAGCGA) at various activation energies. The $M^{+\bullet\bullet}$ ion is generated by electron transfer to the M^{3+} ion in the MS^2 step. The cleavage sites producing the most abundant backbone fragments are indicated in the scheme

However, the impact of the charge distribution on the stability of radical nucleic acids and their dissociation in the gas-phase must be taken into consideration when verifying this hypothesis on radical nucleic acid anions.

The stacking hypothesis was verified by ETD experiments on cationic DNA hexamers harboring abasic sites, using d(TAGCGA) as starting structure. One or both guanines flanking the cytosine were replaced by hydrogen atoms at the C1' of the deoxyribose to obtain d(TAGC_A) and d(TA_C_A), (_ symbolizes abasic sites). ETD experiments on both M^{3+} precursors revealed augmented dissociation yields compared with the original hexamer. The backbone fragments contribute only 1% to the total ion intensity in the ETD spectrum of d(TAGCGA), compared with 25% in d(TAGC_A) and 49% in d(TA_C_A) (compare Table 1 and Figure 6). This trend supports the stacking hypothesis. In d(TA_C_A), the unpaired electron transferred to the cytosine nucleobase is no longer stabilized by the interaction with vicinal guanine nucleobases and, therefore, triggers the fragmentation of the radical cation.

In addition to facilitating fragmentation, the abasic sites also influence the favored cleavage sites. The most abundant

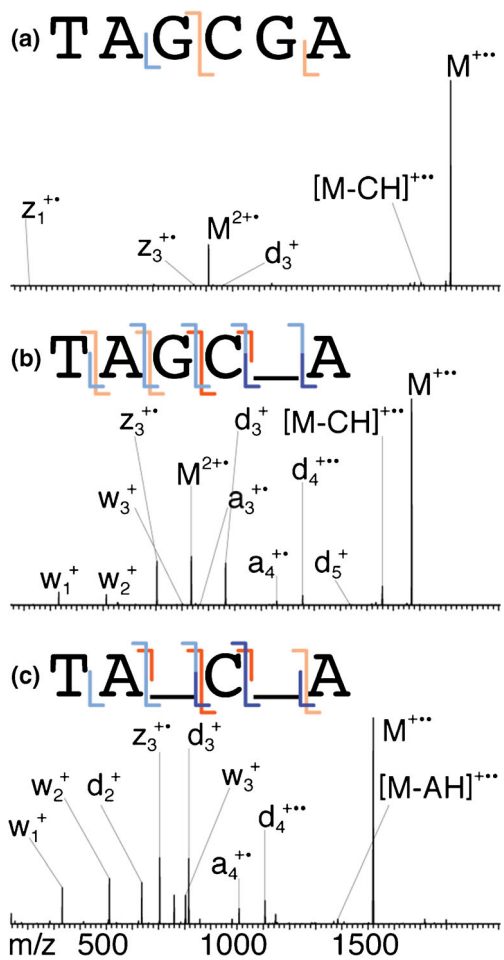

Figure 6. ETD spectra of the DNA hexamers **(a)** d(TAGCGA), **(b)** d(TAGC_A), and **(c)** d(TA_C_A). In the schemes, the formation of a•/w and d/z• pairs are indicated with blue and orange lines, respectively. Pale colors indicate relative ion intensities <0.1%

fragments of d(TAGC_G) are w_1^+, w_2^+, d_3^+, and $z_3^{+\bullet}$ ions, revealing backbone cleavage at the abasic site and the cytidine. Backbone cleavage occurred on both sides of the abasic sites, suggesting that the unpaired electron can be transferred directly to the deoxyribose. In the absence of a nucleobase, the deoxyribose is more accessible for the electron carrier and the protonation of the oxygen atom in the sugar moiety may assist electron transfer. However, the relative ion intensities identify the 5'-C–O bond between G and C as the preferred cleavage site. Introducing the second abasic site in d(TA_C_A) reduces this selectivity. While the $d_3^+/z_3^{+\bullet}$ is still the most abundant ion pair, the corresponding peaks in the ETD spectrum of d(TA_C_A) are less dominant, and the $a_4^{+\bullet}/w_2^+$ pair exhibits comparable intensity. The presence of abasic sites correlates with backbone cleavage on the opposite side of the adjacent cytosine. In other words, the remaining guanine in d(TAGC_A) drives the dissociation towards scission at the phosphate group between G and C.

The propensity and efficiency of π–π-stacking depends on the nucleobases. This has been investigated experimentally and theoretically for dinucleoside monophosphates. According to thermal perturbation differential spectroscopy data, purine–purine pairs exhibit the highest stacking preference, followed by mixed and pyrimidine–pyrimidine pairs [29]. Molecular dynamics simulations, semi-empirical and ab initio calculations later confirmed this trend [30–32]. Consequently, the stacking hypothesis provides an explanation for the different dissociation yields previously reported for the DNA homomers. The low intensity of backbone fragments in the dA_6 and dG_6 spectra is attributed to high stacking efficiencies of the purine nucleobases. In conclusion, the stacking hypothesis rationalizes the fragmentation of charge-reduced DNA oligonucleotides and sugar-modified nucleic acids and presents the more convincing explanation for the stability of DNA radical ions in the gas-phase.

Conclusion

The presented ETD experiments on DNA cations confirm the charge-directed nature of electron transfer evidenced by the selective reduction of cytosine nucleobases in DNA hexamers harboring all four nucleobases. This reduction gives rise to backbone cleavage, preferably at the 5'-C–O bond of the reduced nucleobase. While the main backbone fragments, *a*•, *d*, *w*, and *z*• ions, are the same as previously reported for ECD, the presented ETD data suggest an alternative fragmentation mechanism. Internal electron transfer from the reduced nucleobase induces the scission of a C–O bond in the backbone, resulting in a negative charge on the phosphate linker of the *d*/*w* ion and an unpaired electron on the sugar moiety of the *a*•/*z*• ion. The transfer of hydrogen radicals previously identified as trigger for backbone cleavage in ECD experiments is a minor reaction pathway only, which marks a significant difference between ECD fragmentation patterns and the herein presented ETD data. The proposed mechanism is independent of specific 2'-substituents. This is confirmed by ETD experiments on RNA, methylphosphonate-DNA, and homo-DNA, in which the same

fragmentation patterns were observed as for DNA. Consequently, radical activation techniques harbor great potential for the sequencing of nucleic acids comprising multiple modifications, such as gapmers or tRNAs. Moreover, owing to the preferred reduction of protonated cytosines, ETD data provides sequence information complementary to CID experiments, especially for C-rich sequences.

Two hypotheses are put forward attributing the low dissociation yield of DNA radical cations to non-covalent interactions between complementary fragments or to the stabilization of the unpaired electron in stacked nucleobases. In contradiction to the first hypothesis, high-energy collision-induced dissociation of the $M^{+\bullet\bullet}$ ion results in CID-typical ions, while neither the generation of ETD-typical *a*•/*w* and *d*/*z*• pairs nor preferred cleavage at cytosines were observed. Therefore, the high intensity of the biradical cation is attributed to the stabilization of the unpaired electrons by π–π-stacking. This explanation is in agreement with the ETD data on homo-DNA oligonucleotides and correctly predicts the effect of abasic sites on the fragmentation of a DNA hexamer.

Acknowledgments

The authors thank Professor Dr. Kathrin Breuker for the fruitful discussions of the present work.

References

1. McLuckey, S.A., Van Berkel, G.J., Glish, G.L.: Tandem mass spectrometry of small, multiply charged oligonucleotides. J. Am. Soc. Mass Spectrom. **3**, 60–70 (1992)
2. Wu, J., McLuckey, S.A.: Gas-phase fragmentation of oligonucleotide ions. Int. J. Mass Spectrom. **237**, 197–241 (2004)
3. Schürch, S.: Characterization of nucleic acids by tandem mass spectrometry - the second decade (2004–2013): from DNA to RNA and modified sequences. Mass Spectrom. Rev. **35**, 483–523 (2016)
4. Håkansson, K., Hudgins, R.R., Marshall, A.G., O'Hair, R.A.J.: Electron capture dissociation and infrared multiphoton dissociation of oligodeoxynucleotide dications. J. Am. Soc. Mass Spectrom. **14**, 23–41 (2003)
5. Schultz, K.N., Håkansson, K.: Rapid electron capture dissociation of mass-selectively accumulated oligodeoxynucleotide dications. Int. J. Mass Spectrom. **234**, 123–130 (2004)
6. Chan, T.W.D., Choy, M.F., Chan, W.Y.K., Fung, Y.M.E.: A mechanistic study of the electron capture dissociation of oligonucleotides. J. Am. Soc. Mass Spectrom. **20**, 213–226 (2009)
7. Smith, S.I., Brodbelt, J.S.: Electron transfer dissociation of oligonucleotide cations. Int. J. Mass Spectrom. **283**, 85–93 (2009)
8. Yang, J., Mo, J., Adamson, J.T., Håkansson, K.: Characterization of oligodeoxynucleotides by electron detachment dissociation Fourier transform ion cyclotron resonance mass spectrometry. Anal. Chem. **77**, 1876–1882 (2005)
9. Kinet, C., Gabelica, V., Balbeur, D., De Pauw, E.: Electron detachment dissociation (EDD) pathways in oligonucleotides. Int. J. Mass Spectrom. **283**, 206–213 (2009)
10. McLuckey, S.A., Stephenson, J.L., O'Hair, R.A.J.: Decompositions of odd- and even-electron anions derived from deoxy-polyadenylates. J. Am. Soc. Mass Spectrom. **8**, 148–154 (1997)
11. Gao, Y., McLuckey, S.A.: Electron transfer followed by collision-induced dissociation (NET-CID) for generating sequence information from backbone-modified oligonucleotide anions. Rapid Commun. Mass Spectrom. **27**, 249–257 (2013)
12. Gabelica, V., Tabarin, T., Antoine, R., Rosu, F., Compagnon, I., Broyer, M., De Pauw, E., Dugourd, P.: Electron photodetachment dissociation of DNA polyanions in a quadrupole ion trap mass spectrometer. Anal. Chem. **78**, 6564–6572 (2006)
13. Yang, J., Håkansson, K.: Characterization of oligodeoxynucleotide fragmentation pathways in infrared multiphoton dissociation and electron detachment dissociation by Fourier transform ion cyclotron double resonance. Eur. J. Mass Spectrom. **15**, 293–304 (2009)
14. Horn, D.M., Ge, Y., McLafferty, F.W.: Activated ion electron capture dissociation for mass spectral sequencing of larger (42 kDa) proteins. Anal. Chem. **72**, 4778–4784 (2000)
15. Horn, D.M., Breuker, K., Frank, A.J., McLafferty, F.W.: Kinetic intermediates in the folding of gaseous protein ions characterized by electron capture dissociation mass spectrometry. J. Am. Chem. Soc. **123**, 9792–9799 (2001)
16. Breuker, K., Oh, H.B., Horn, D.M., Cerda, B.A., McLafferty, F.W.: Detailed unfolding and folding of gaseous ubiquitin ions characterized by electron capture dissociation. J. Am. Chem. Soc. **124**, 6407–6420 (2002)
17. Yang, J., Håkansson, K.: Fragmentation of oligoribonucleotides from gas-phase ion-electron reactions. J. Am. Soc. Mass Spectrom. **17**, 1369–1375 (2006)
18. Green-Church, K.B., Limbach, P.A.: Mononucleotide gas-phase proton affinities as determined by the kinetic method. J. Am. Soc. Mass Spectrom. **11**, 24–32 (2000)
19. Arcella, A., Dreyer, J., Ippoliti, E., Ivani, I., Portella, G., Gabelica, V., Carloni, P., Orozco, M.: Structure and dynamics of oligonucleotides in the gas phase. Angew. Chem. Int. Ed. **54**, 467–471 (2015)
20. Green-Church, K.B., Limbach, P.A., Freitas, M.A., Marshall, A.G.: Gas-phase hydrogen/deuterium exchange of positively charged mononucleotides by use of fourier-transform ion cyclotron resonance mass spectrometry. J. Am. Soc. Mass Spectrom. **12**, 268–277 (2001)
21. Riml, C., Glasner, H., Rodgers, M.T., Micura, R., Breuker, K.: On the mechanism of RNA phosphodiester backbone cleavage in the absence of solvent. Nucleic Acids Res. **43**, 5171–5181 (2015)
22. Böhringer, M., Roth, H.J., Hunziker, J., Göbel, M., Krishnan, R., Giger, A., Schweizer, B., Schreiber, J., Leumann, C., Eschenmoser, A.: Why pentose and not hexose nucleic-acids? Part II. Preparation of oligonucleotides containing 2',3'-dideoxy-b-D-glucopyranosyl building blocks. Helv. Chim. Acta. **75**, 1416–1477 (1992)
23. Nyakas, A., Blum, L.C., Stucki, S.R., Reymond, J.-L., Schürch, S.: OMA and OPA—software-supported mass spectra analysis of native and modified nucleic acids. J. Am. Soc. Mass Spectrom. **24**, 249–256 (2013)
24. Berdys, J., Skurski, P., Simons, J.: Damage to model DNA fragments by 0.25–1.0 eV electrons attached to a thymine π* orbital. J. Phys. Chem. B. **108**, 5800–5805 (2004)
25. Stucki, S.R., Désiron, C., Nyakas, A., Marti, S., Leumann, C.J., Schürch, S.: Gas-phase dissociation of homo-DNA oligonucleotides. J. Am. Soc. Mass Spectrom. **24**, 1997–2006 (2013)
26. Glasner, H., Riml, C., Falschlunger, C., Micura, R., Breuker, K.: Characterization of intramolecular nucleobase–phosphate interactions by site-specific nucleobase methylation and collisionally activated dissociation. Proceedings of 65th ASMS Conference on Mass Spectrometry and Allied Topics, Indianapolis, IN, June 4–8 (2017)
27. Egli, M., Lubini, P., Pallan, P.S.: The long and winding road to the structure of homo-DNA. Chem. Soc. Rev. **36**, 31–45 (2007)
28. Anusiewicz, I., Berdys, J., Sobczyk, M., Skurski, P., Simons, J.: Effects of base π-stacking on damage to DNA by low-energy electrons. J. Phys. Chem. A. **108**, 11381–11387 (2004)
29. Frechet, D., Ehrlich, R., Remy, P., Gabarro-Arpa, J.: Thermal perturbation differential spectra of ribonucleic-acids. II. Nearest neighbor interactions. Nucleic Acids Res. **7**, 1981–2001 (1979)
30. Šponer, J., Leszczyński, J., Hobza, P.: Nature of nucleic acid-base stacking: nonempirical ab initio and empirical potential characterization of 10 stacked base dimers. Comparison of stacked and H-bonded base pairs. J. Phys. Chem. **100**, 5590–5596 (1996)
31. Norberg, J., Nilsson, L.: Stacking free-energy profiles for all 16 natural ribodinucleoside monophosphates in aqueous solution. J. Am. Chem. Soc. **117**, 10832–10840 (1995)
32. Šponer, J., Leszczynski, J., Hobza, P.: Electronic properties, hydrogen bonding, stacking, and cation binding of DNA and RNA bases. Biopolymers. **61**, 3–31 (2001)